Emerging coherence with unified energy, temperature, and lifetime scale in heavy fermion YbRh_{2}Si_{2}

S.-K. Mo, W. S. Lee, F. Schmitt, Y. L. Chen, D. H. Lu, C. Capan, D. J. Kim, Z. Fisk, C.-Q. Zhang, Z. Hussain, and Z.-X. Shen

Phys. Rev. B **85**, 241103 — Published 22 June 2012

DOI: 10.1103/PhysRevB.85.241103

Emerging coherence with unified energy, temperature and lifetime scale in heavy fermion $YbRh_2Si_2$

S.-K. Mo*,[1,2] W. S. Lee,[2,3] F. Schmitt,[2,3] Y. L. Chen,[2,3] D. H. Lu,[2,3] C. Capan,[4] D. J. Kim,[4] Z. Fisk,[4] C.-Q. Zhang,[5] Z. Hussain,[1] and Z.-X. Shen†[2,3]

[1]*Advanced Light Source, Lawrence Berkeley National Laboratory, Berkeley, CA 94720*
[2]*Geballe Laboratory for Advanced Materials, Department of Physics and Applied Physics, Stanford University, Stanford, CA 94305*
[3]*Stanford Institute for Materials and Energy Sciences, SLAC National Accelerator Laboratory, 2575 Sand Hill Road, Menlo Park, CA 94025*
[4]*Department of Physics and Astronomy, University of California, Irvine, CA 92697*
[5]*State Key Laboratory of Crystal Materials, Shandong University, Jinan, 250100, China*

(Dated: Received)

We present ultra-high resolution angle-resolved photoemission data of prototypical Kondo lattice system $YbRh_2Si_2$, using 7eV laser photon source. Detailed temperature dependent measurements reveal the development of coherent states, in the form of sharp weakly dispersing peaks at the lowest energy of single-electron spectra, below a characteristic temperature. The characteristic temperature, obtained from angle-resolved photoemission, is intriguingly of exactly the same scale as the energy and the lifetime of the coherent state.

PACS numbers: 71.20.Eh, 71.27.+a, 79.60.-i

The single-ion Kondo description of the heavy fermion phenomena provides a theoretical background to understand the spectroscopic and thermodynamic properties of a number of Ce, Yb and U based intermetallics [1–3]. The interaction between the local magnetic moments of the f-electrons and the conduction electrons results in a many-body singlet ground state, the Kondo resonance, with binding energy k_BT_K, which accompanies a loss of the local moments below T_K and the enhancement of the quasiparticle effective mass. The single-ion Kondo temperature, T_K, is the only relevant temperature scale. Connecting the single-ion description to a more realistic theory that accounts for the array of local moments in a crystal, the Kondo lattice, has been proven to be a challenging problem due to the complex interplay between the local Kondo interaction and the intersite Ruderman-Kittel-Kasuya-Yoshida (RKKY) coupling. Various theoretical studies [1, 4–8] suggest the existence of a characteristic temperature T^* that assumes the role of T_K. However, the relationship between T^* and T_K, and the details of changes in the electronic structure across T^* has not been completely clear. This difficulty has been compounded by the lack of spectroscopic data with sufficient resolution and covering wide range of temperature to address these issues.

Photoemission spectroscopy (PES) has played a crucial role in the development of the single-ion Kondo scenario by directly measuring sharp Kondo resonance peak, extracting interaction parameters and comparing them to thermodynamic properties [3, 9, 10]. An analogous approach to the Kondo lattice problem demands a fully momentum resolved single-electron spectral function, measured by angle-resolved PES (ARPES) [11], in the vicinity of very low binding energy comparable to k_BT^*, typically within 10 meV below E_F. Given the typical low temperature scale involved in a heavy fermion system, measuring such a small dispersion of coherent states close to E_F has been a challenge due to insufficient energy and momentum resolution. So far, literature is sparse and they typically show only the intensity variation for near E_F peaks [12, 13] or the hybridization features deeper in binding energy [14]. They were generally measured with photon energies larger than 100 eV at the $4d$-$4f$ edge [15, 16], at which the momentum resolution is intrinsically limited and the energy resolution is limited by the performance of synchrotron sources. More importantly, not many high-resolution temperature dependent data is available except across the hidden order transition in URu_2Si_2 [17].

To gaining further insight into the Kondo lattice problems in the energy-momentum space within the energy scale of the k_BT^*, this Rapid Communication reports ultra-high resolution laser ARPES data using photons with an energy of 7 eV on $YbRh_2Si_2$, a Kondo lattice compounds [18] in the vicinity of quantum critical point [19] (QCP). 7 eV laser photon source is ideal and essential for exploring such small dispersions due to the markedly better resolutions compared to previous studies, with energy resolution of 3 meV and momentum resolution of 0.003 $Å^{-1}$, and with hitherto unexplored sensitivity of f spectral weight at extremely low photon energies. $YbRh_2Si_2$ is a particularly appropriate system for such investigations because the heavy coherent state in Yb compounds lies right below $E_F$and thus reachable by photoemission [4, 9, 10], not above as in Ce equivalents. Furthermore, the main f-related features in ARPES lie near the Γ-point [20–22] that can be reached within the accessible momentum-(k-)space for such small photon en-

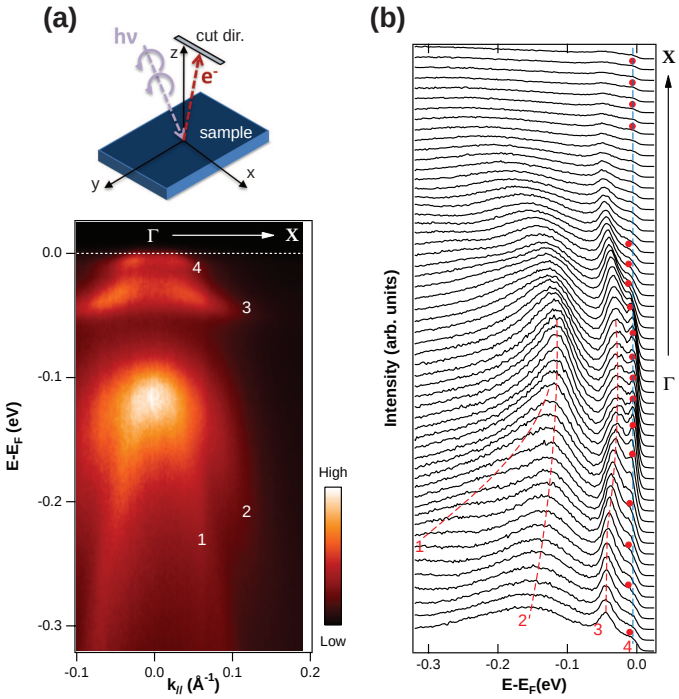

FIG. 1: (Color Online) Angle resolved photoemission spectra of $YbRh_2Si_2$ measured with 7 eV laser. (a) ARPES data were taken along the Γ-X direction of the projected body centered tetragonal Brillouin zone at $T = 12$ K with a geometry shown in the schematic diagram. Circularly polarized light was used and the cut direction is depicted as a strip. Bands are labeled as 1 - 4 in (a). Energy distribution curves from the same data set as in (a) are shown in (b). The red (dark gray) dashed lines are added to guide eyes to bands 1 - 3. The red (dark gray) dots follow the band 4. The blue (gray) dashed line shows the position of the binding energy of the flat part in band 4.

ergy.

Single crystals of $YbRh_2Si_2$ have been grown using the flux method as described in Ref. [23]. ARPES measurements were carried out at Stanford University equipped with 7 eV laser photon source and a SES 2002 electron analyzer. The total energy resolution was set to be 3 meV and the angular resolution was 0.2°. The latter corresponds to less than 1% of the length of the Brillouin zone. Well-oriented single crystals were cleaved in situ and measured with a base pressure better than 3×10^{-11} Torr. The quality of the sample surface was monitored by continually measuring reference spectra. All the data presented here were measured within 24 hours after cleave and showed minimal surface degradation.

Fig. 1 shows the overall ARPES spectra along Γ-X. The dispersing features labelled as 1 - 3 agree very well with those shown in the data taken with 55 eV synchrotron light in a similar geometry [21], albeit not with LDA calculations [24]. Even though calculation is not available for low excitation energy, it has been shown experimentally [25, 26] that photoionization cross-sections of $4f$ states are sufficient for low photon energy studies. The features dominating the low energy spectrum (band 3 and 4) locates at consistent energy positions as in Ref. [22], although we do not clearly observe the crystal-field split sub-bands between these two states. Also suppressed are the near E_F features found in Ref. [21] away from Γ-point ($k \gtrsim 0.15$ Å^{-1}). We attribute these to the unique matrix elements of our experimental setup and the use of very low photon energy of 7 eV. The nearly flat feature at the lowest energy (band 4) is nonetheless very clear and it is our main focus for this paper. Fig. 1(b) shows the energy distribution curves (EDCs) along the same cut shown in Fig. 1(a). The sharp quasiparticle (QP) peaks are evident and their peak positions are right below E_F. They are rather dispersionless near the Γ-point with peak positions roughly at 4 meV and start dispersing to higher binding energy from $k \sim 0.03$ Å^{-1}. One also notice that the peak positions farther away from the Γ-point, though the intensity is heavily suppressed, are back at 4 meV.

The dispersion relation of the QP peaks is better shown in Fig. 2, where we present the second derivative of the intensity map and dispersion relation extracted from the peak positions obtained from EDCs using the data shown in Fig. 1. There exists a sharp crossover, within a single band, from a dispersionless region around the Γ-point to dispersing peaks away from it. As shown in the fitting lines in Fig. 2(c) and schematic diagrams in Figs. 2(d), the natural way to explain this rather disjoint dispersion in a single band is that we observe the dominating f-branch, which is very flat and lies slightly below E_F around the Γ-point. It hybridizes with the more dispersive band seen in higher binding energy, consequently mixing partial f-weight into the Fermi surface for the other branch observed for $k > 0.05$ Å^{-1} though its weight is heavily suppressed.

We now turn our attention to the temperature dependence of the ARPES data. Fig. 3 shows the ARPES data along the same high symmetry line as in Fig. 1(a) for a few selected temperatures. A full data set with more temperature steps is available as supplementary information. The data shown here are reproducible with minimal sample surface degradation during a low-high-low temperature cycle. The QP peaks are clear at $T = 12$ K, but their intensity become weaker as temperature increases. At $T = 45$ K, the QP peaks become hard to distinguish from the Fermi edge, and they get completely washed away by the thermal broadening at $T = 110$ K. While the QP peaks becomes weaker with increasing temperature, the previously identified high energy peaks around 30 meV and 110 meV do not show much change besides the trivial thermal broadening.

For more detailed analysis, we have picked out EDCs at $k \sim 0.03$ Å^{-1}, the onset of the flat part of the QP band, as shown in Fig 4(a). It is clear the peak height

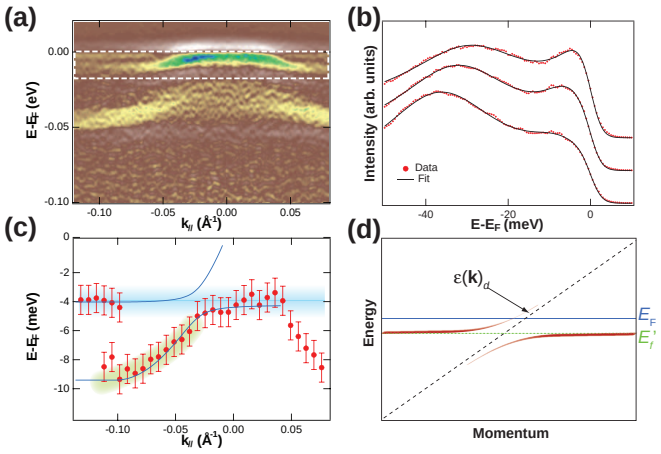

FIG. 2: (Color Online) Energy vs. momentum dispersion from 2nd derivatives of the intensity map and EDC fits. (a) The 2nd derivative of ARPES data shown in Fig. 1 to enhance the visibility of weak features away from the Γ-point, particularly for $k > 0.05$ Å^{-1}. The white dashed box indicates the blown-up region shown in (c), where the dispersion relation extracted from EDC fits of Fig. 1(b), as exemplified in (b), is presented. The fits are made with 2 Lorentzian peaks added by exponential background to account for the tail from high binding energy peak, which is then multiplied by Fermi function and convoluted by Gaussian to include experimental resolution. Samples of the fit are shown in panel (b) for k = -0.10, -0.05 and 0.02 Å^{-1}. In panel (c), blue (gray) and green (light gray) shades are added as guides to eyes for the flat and dispersing features, respectively. Blue (gray) lines show the best fit of the dispersion relation using slave boson treatment of the periodic Anderson model (Ref. [16]). (d) Schematic diagram explaining energy-momentum dispersion relation of f-d hybridized state (red curves) close to E_F under periodic Anderson model (See, for example, Ref. [4] and [15]), with schematic representation of spectral weight of states of f-character. Thicker part of the curves implies higher intensity in the spectral function. E_f' denotes the energy level of the renormalized f-state and $\epsilon(k)_d$ (black dashed line) is the bare dispersion of the original d band. Note that the position of the E_f' lies below E_F following the electron-hole symmetry of Ce and Yb systems.

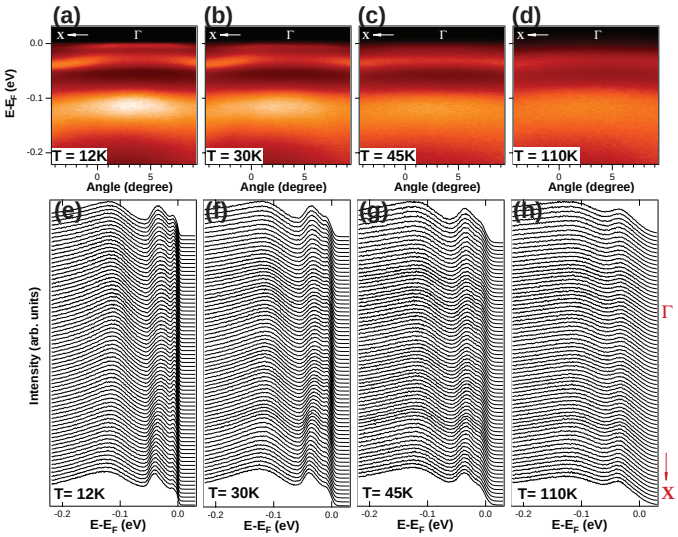

FIG. 3: (Color Online) Temperature dependence of the ARPES spectra along Γ-X direction. (a) - (d) Intensity plots at T = 12, 30, 45 and 110 K. The color scale is the same as in Fig. 1. (e) - (h) EDCs corresponding (a) - (d). The temperature was cycled from low to high and back to low temperatures to verify that changes in spectra are not due to a trivial surface degradation.

and the peak weight decreases with increasing temperature. However, it is hard to distinguish the temperature dependence with the thermal broadening since the QP peaks are well within the $4k_BT$ range. To separate the trivial thermal effect from the temperature dependence of the spectral function, the Fermi-Dirac divided spectra are shown in Fig. 4(b). The spectra are essentially flat close to E_F for $T > 45$ K, indicating that the sharp peak close to E_F emerges only below this temperature. More importantly, we observe that the uprise of Fermi-Dirac divided weight above E_F is only observed below the same temperature, which may indicate another branch of the QP peak above E_F also follows the same temperature dependence. This overall change in the spectral structure (blue (gray) to red (dark gray) shade in Fig. 4(b)) provide us the way to define the characteristic temperature of $YbRh_2Si_2$ obtained by ARPES. We have repeated the same measurements and analysis with 3 different samples of $YbRh_2Si_2$ and the results are consistent except minor differences in the onset temperature at which the QP peaks start to get suppressed. Fig. 4(c) summarize the whole data set by showing the relative weight of the QP peaks. The weight has been evaluated from a simple integration for the energy window of the QP peak, i.e. energy above the dip between the QP peak and the next high binding energy peak, since the fitting procedure shown in Fig. 2 is not possible for high temperature data, for which the QP peaks are completely washed out.

The general trend qualitatively agrees with the prediction from Ref. [5] and [27], a logarithmic decrease in peak height as temperature increases with an onset temperature $\sim T^*$. This rather dramatic temperature dependence is much different from that of crystal field split excitations [28]. The onset of the QP peak development is estimated as $T^*_{\rm ARPES} = 50 \pm 10$ K, which is much higher than $T_K \sim 25 \pm 5$ K from thermodynamic measurement [8, 23, 29]. A small decrease of the peak intensity caused by the minor sample degradation over time, in the same direction as increasing temperature, makes $T^*_{\rm ARPES}$ a lower bound estimate. It is interesting to note that our $T^*_{\rm ARPES}$ value is in good agreement with that estimated from spectroscopic and thermodynamic measurements combined with a simple scaling theory [8]. Recent scanning tunneling spectroscopy measurement [30] also finds the lowest energy excitation follows a similar

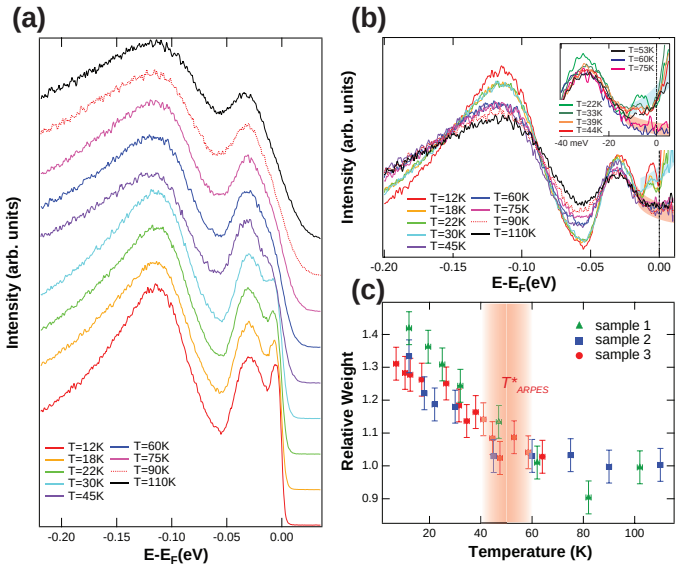

FIG. 4: (Color Online) Detailed analysis on temperature dependent ARPES spectra. (a) EDCs at the same k-point, $k \sim 0.03$ Å^{-1}, the onset of the flat part of the dispersion in Fig. 2, at different temperatures. (b) The spectra in (a) divided by Fermi-Dirac function convolved with Gaussian of width comparable to experimental resolution to remove the thermal broadening contribution in the spectral change. The panel shows wide range data set. The inset focuses on most interesting temperature and energy ranges. (c) The relative quasiparticle spectral weight calculated by integrating spectral weight only for the energy window for the quasiparticle peak (-15 meV and above) and divided by the weight from high temperature value of $T = 110$ K data. The measurement was repeated with three different samples of $YbRh_2Si_2$ with slightly different temperatures and the results are highly reproducible as shown in the Figure. $T^*_{\rm ARPES}$ is indicated as red shade.

temperature dependence.

Our data show a non-trivial development of changes in the low energy electronic structure of $YbRh_2Si_2$, at an onset temperature well above $T_{\rm K}$. More interestingly, the peak position and the width of the QP states corresponds approximately to $k_B T^*_{\rm ARPES} \sim 4$ meV, just as if T^* replaces $T_{\rm K}$ in the conventional single-ion description of the spectral function for heavy fermion systems. However, the important difference is that this energetics even applies to a single EDC at a particular k-value, not just to the k-integrated PES spectra as in the single-ion case. Most importantly, this provides a rare spectroscopic evidence in a Kondo system where three aspects of the spectroscopic energy scales, the binding energy, the width and thus the lifetime, as well as the coherence temperature, collapse into a single temperature scale. The emergence of a coherent state with such a unified scale for many aspects of the physical properties is likely a consequence of profound underlying physics.

Another important aspect of our data is that it shows the development of QP states even in the vicinity of a QCP, where thermodynamic properties show non-Fermi liquid behaviors at low temperatures [19]. This furnishes intriguing insight for the systems that have been studied in relation to QCP, such as high-T_c cuprates [31], in which the emergence of QP like peaks can still be observed near the underlying Fermi surface despite the non-Fermi liquid property exemplified by T-linear resistivity.

In summary, we have discovered a dramatic temperature dependence of the lowest-lying excitations in the single-particle spectral function of a Kondo lattice system $YbRh_2Si_2$. The characteristic temperature obtained from the ARPES measurement scales very well with other two energy scales of the system, the peak position and the width of the peak. Our discovery provides significant insight into the low energy electronic structure of a Kondo lattice going beyond the single-ion model. It also sets informative constraints in the future development of Kondo lattice understanding of heavy fermion compounds.

We thank J. W. Allen, F. Steglich and P. Coleman for inspiring discussions. The work at Stanford is supported by National Science Foundation (DMR-0604701) for S.-K. Mo, and the work at SIMES and SLAC National Accelerator Laboratory is supported by the Office of Basic Energy Sciences of the U.S. Department of Energy (DE-AC02-76SF00515). The Advanced Light Source is supported by the Office of Basic Energy Sciences of the U.S. Department of Energy (DE-AC02-05CH11231). The work at the UCI is supported by the U.S. National Science Foundation (DMR-0801253).

*SKMo@lbl.gov
†zxshen@stanford.edu

[1] P. Coleman, in *Handbook of Magnetism and Advanced Magnetic Materials* edited by H. Kronmüller and S. Parkin (Wiley, 2007).

[2] A. C. Hewson, *The Kondo Problem to Heavy Fermions* (Cambridge University Press, 1993).

[3] O. Gunnarsson and K. Shoenhammer in *Handbook on the Physics and Chemistry of Rare Earths* **10**, 103 (1987).

[4] A. N. Tahvildar-Zadeh, M. Jarrell, and J. K. Freericks, Phys. Rev. Lett. **80**, 5168 (1998).

[5] J. H. Shim, K. Haule and G. Kotliar, Science **318**, 1615-1617 (2007).

[6] J. Otsuki, H. Kusunose and Y. Kuramoto, Phys. Rev. Lett. **102**, 017202 (2009).

[7] S. Nakatsuji, D. Pines and Z. Fisk, Phys. Rev. Lett. **92** 016401 (2004).

[8] Y.-F. Yang, Z. Fisk, H.-O. Lee, J. D. Thompson and D. Pines, Nature **454**, 611 (2008).

[9] J. W. Allen, S. J. Oh, O. Gunnarsson, K. Schönhammer, M. B. Maple, M. S. Torikachvili and I. Lindau, Adv. Phys. **35**, 275 (1986).

[10] D. Malterre, M. Grioni and Y. Baer, Adv. Phys. **45**, 299 (1996).

[11] A. Damascelli, Z. Hussain and Z.-X. Shen, Rev. Mod. Phys. **75**, 473 (2003).

[12] S.-I. Fujimori, A. Fujimori, K. Shimada, T. Narimura, K. Kobayashi, H. Namatame, M. Taniguchi, H. Harima, H. Shishido, S. Ikeda, D. Aoki, Y. Tokiwa, Y. Haga and Y. Ōnuki, Phys. Rev. B **73**, 224517 (2006).

[13] S. Danzenbächer, Yu. Kucherenko, M. Heber, D. V. Vyalikh, S. L. Molodtsov, V. D. P. Servedio and C. Laubschat, Phys. Rev. B **72**, 033104 (2005).

[14] S. Danzenbächer, Yu. Kucherenko, C. Laubschat, D. V. Vyalikh, Z. Hossain, C. Geibel, X. J. Zhou, W. L. Yang, N. Mannella, Z. Hussain, Z.-X. Shen and S. L. Molodtsov, Phys. Rev. Lett. **96**, 106402 (2006).

[15] J. D. Denlinger, G.-H. Gweon, J. W. Allen, C. G. Olson, M. B. Maple, J. L. Sarrao, P. E. Armstrong, Z. Fisk and H. Yamagami, J. Electron. Spectrosc. Relat. Phenom. **117**, 347 (2001).

[16] H. J. Im, T. Ito, H.-D. Kim, S. Kimura, K. E. Lee, J. B. Hong, Y. S. Kwon, A. Yasui and H. Yamagami, Phys. Rev. Lett. **100**, 176402 (2008).

[17] A. F. Santander-Syro, M. Klein, F. L. Boariu, A. Nuber, P. Lejay and F. Reinert, Nature Phys. **5**, 637-641 (2009).

[18] P. Gegenwart, Y. Tokiwa, T. Westerkamp, F. Weickert, J. Custers, J. Ferstl, C. Krellner, C. Geibel, P. Kerschl, K.-H. Mueller and F. Steglich, New J. Phys. **8**, 171 (2006).

[19] P. Gegenwart, Q. Si and F. Steglich, Nat. Phys. **4** 186 (2008).

[20] G. A. Wigger, F. Baumberger, Z.-X. Shen, Z. P. Yin, W. E. Pickett, S. Maquilon and Z. Fisk, Phys. Rev. B **76**, 035106 (2007).

[21] D. V. Vyalikh, S. Dänzenbacher, A. N. Yaresko, M. Holder, Yu. Kucherenko, C. Laubschat, C. Krellner, Z. Hossain, C. Geibel, M. Shi, L. Patthey and S. L. Molodtsov Phys. Rev. Lett. **100**, 056402 (2008).

[22] D. V. Vyalikh , S. Dänzenbacher, Yu. Kucherenko, K. Kummer, C. Krellner, C. Geibel, M. G. Holder, T. K. Kim, C. Laubschat, M. Shi, L. Patthey, R. Follath and S. L. Molodtsov, Phys. Rev. Lett. **105**, 237601 (2010).

[23] U. Köhler, N. Oeschler, F. Steglich, S. Maquilon and Z. Fisk, Phys. Rev. B **77**, 104412 (2008).

[24] T. Jeong, J. Phys.: Condens. Matter **18**, 6289 (2006).

[25] M. Matsunami, R. Eguchi, T. Kiss, K. Horiba, A. Chainani, M. Taguchi, K. Yamamoto, T. Togashi, S. Watanabe, X.-Y. Wang, C.-T. Chen, Y. Senba, H. Ohashi, H. Sugawara, H. Sato, H. Harima and S. Shin, Phys. Rev. Lett. **102**, 036403 (2009).

[26] S. L. Friedman, Ph. D. Dissertation, Stanford University (2000).

[27] Y.-F. Yang and D. Pines, Phys. Rev. Lett. **100**, 096404 (2008).

[28] D. Ehm, S. Hüfner, J. Kroha, P. Wölfle, O. Stockert, C. Geibel and H. V. Löhneysen, Phys. Rev. B **76** 045117 (2007).

[29] O. Trovarelli, C. Geibel, S. Mederle, C. Langhammer, F. M. Grosche, P. Gegenwart, M. Lang, G. Sparn and F. Steglich, Phys. Rev. Lett. **85**, 626 (2000).

[30] S. Ernst, S. Kirchner, C. Krellner, C. Geibel, G. Zwicknagl, F. Steglich and S. Wirth, Nature **474**, 362 (2011).

[31] S. Sachdev, Rev. Mod. Phys. **75**, 913 (2003).